**SUPPLEMENTARY DATA IN SIX PARTS (Pindell & Heyn, 2022, Geol. Soc. Lon.)**

Part A. Ethiopia Cross section.
Part B. Extended caption for Figure 3 of the Text.
Part C. Igneous age compilations, central South Atlantic, providing detail for Figure 6.
Part D. Additional seismic reflection data, Gulf of Mexico.
Part E. Igneous age compilations, Gulf of Mexico, providing detail for Figure 8.
Part F. Iceland as a quasi-analogue for the São Paulo Plateau

**Supplementary Data, Part A. Cross section, Main Ethiopian Rift.**

**Supplementary Data, Fig. A1.** Radar image of the Ethiopian region (see location in **Fig. 2**) showing the elevation profile along the indicated section across the dynamic high, modified from Sembroni et al. (2016). Central Main Ethiopian Rift (MER) is a local low due to tectonic subsidence but remains above sea level (+1000 m) due to the greater regional dynamic uplift. Active magma-rich rifting dominates the central portion of the section but diminishes outward in both directions. The smooth dashed white line below the black section location line shows an idealized estimate of future dynamic subsidence (dissipation of dynamic uplift) if the upward dynamic force from the plume were removed. We show a moderate magnitude that reaches 1.5 km in the centre, but the dynamic subsidence could be even greater. Because erosion and extensional faulting are strong (see topographic profile), we expect the area of today's uplift would be negative after the dissipation.

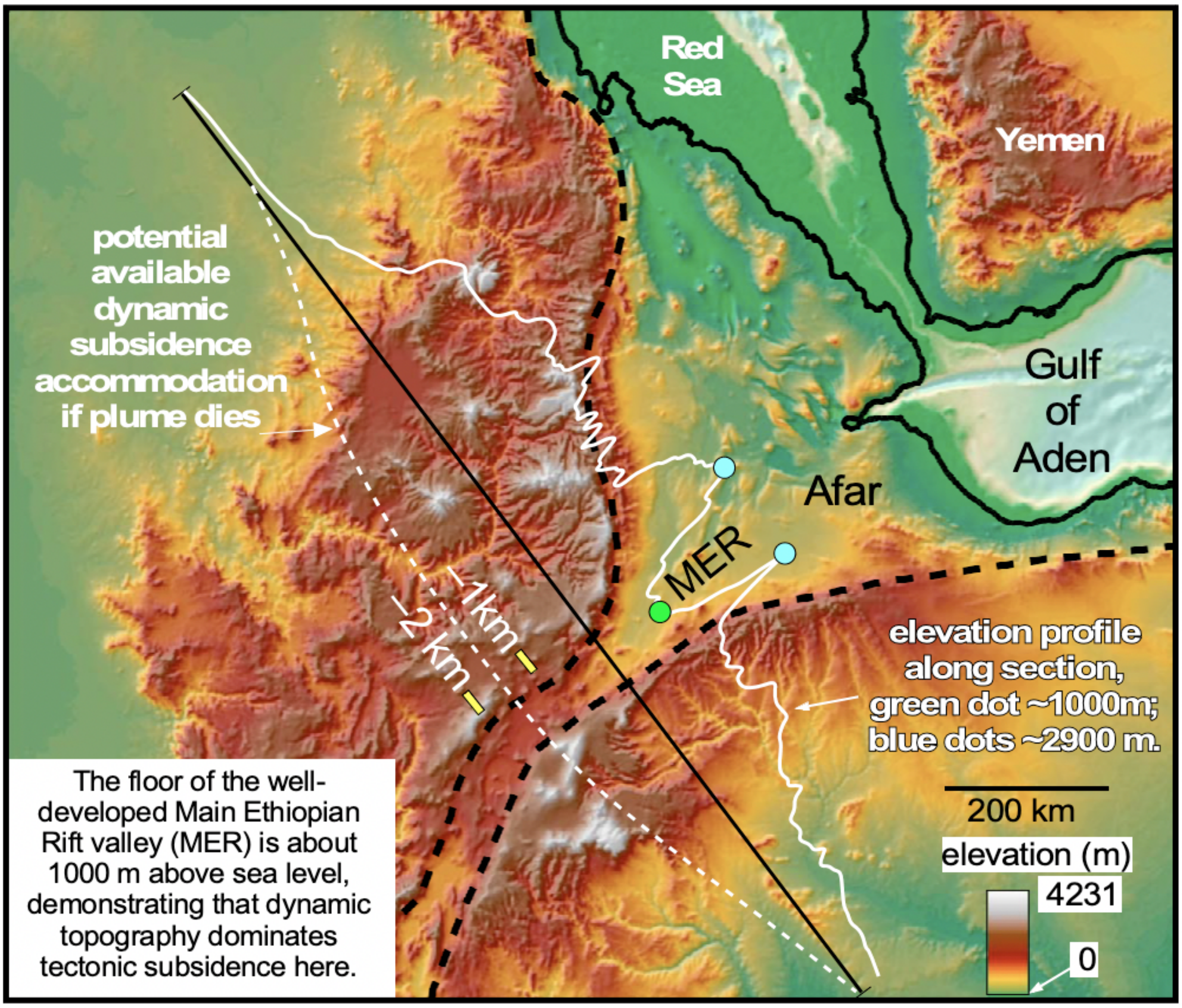

**Supplementary Data, Part B. Extended caption for Figure 3 of the text.**

Lithosphere–plume interactions. Lithosphere, beige; aesthenosphere, grey; magma-rich active rifting, red; areas already rifted but moving off the plume, rose. Pluton shapes (pink) signify complex magmatism at hotspots and magmatic segments (Ebinger and Casey 2001; Ebinger et al. 2017), white where magmatism is only rarely active. Beige arrows show sediment dispersal, flowing outward early on but then inward or in-situ when early accommodation develops. (**a**) Diachronous evolution of a point tracked by black arrows on a plate migrating over a quasi-stationary plume. Dynamic uplift is augmented by isostatic response to surface erosion and to thermal thinning of the base lithosphere. At time T1, marine sedimentation at water depth Y; time T2, shallowing, regressive sedimentation, offlap; T3, hot spot magmatism, thermal thinning of the base lithosphere and crustal thinning by surface erosion, with local subaerial deposition in lows (not shown); T4, end of most magmatism (white remnant diapirs), beginning of dynamic subsidence (dissipation of dynamic uplift) and thermal re-equilibration of base lithosphere (as shown only at base lithosphere in b4), with marine transgression and onlap onto eroded/magmatic surface; T5, return to basinal deposition (yellow), with the erosional unconformity Z deeper than Y due to erosional thinning; T6, continued marine sedimentation with sporadic record of former hot spot magmatism. (**b0–b4**) Symmetrical formation and migration of magma-rich conjugate margins over and off a stationary plume. (**b0**) Early stage of plume, with general uplift, flood basalt eruption and magmatic intrusion, initial outward transport of eroded sediments. (**b1**) Early magma-rich rifting (red) between two future plates with symmetrical displacement off a fixed central plume. Dynamic uplift and thermal erosion (thinning) of base lithosphere keep rift surface above sea level while lithosphere thins. Point P1 was once on the rift crest at P2 but is being displaced off the plume flank by lithospheric extension and magmatic addition. Both dynamic and thermal subsidence will begin near P1. (**b2**) Black and grey faults are active and inactive, marking zones of continued rifting (red) and rifted crust (rose), respectively. Point now marks the central sag basin undergoing both dynamic and thermal subsidence, where little further faulting or magmatism occurs, having moved off the plume flank. Sediment transport is split outward and inward depending on height and continuity of rift shoulders. P2 marks sag or salt section onlap onto the active central magma-rich rift high (P3), which is kept elevated by dynamic uplift. At some settings, magmatism (red zone) overwhelms thinning crust to create thick magmatic crust and further widening of the margins after actual continental breakup has occurred. At the hinge line, post-rift onlap occurs onto full-thickness continental crust which is drawn downward by flexural loading. (**b3**) Both margins are approaching their full tectono-magmatic extension. The central magmatic rift axis will fall below global sea level when tectonic subsidence of continental or magmatic crust dominates dynamic uplift, which is beginning to wane as more normal seafloor spreading is imminent. Transition from sag (yellow) to salt (dark pink) marks either a palaeogeographic connection of the basins to the world ocean, or subsidence below global sea level. Sag/salt section (now salt in **b3**) continues to onlap central magma-rich rift high and eventually buries it as it founders by rifting. P1 is receiving salt above the sag; P2 had marked the sag section onlap limit onto the central rift in **b2**, but is now downfaulted because it was at the former limit of rifting; P3 has only salt which is faulted with basement, and will undergo some syn-rift subsidence and then dynamo-thermal subsidence, potentially producing the thickest salt accumulation along the whole margin; P4 is where the magmatic crust will breakup and transition to seafloor spreading. If available, sediment transport begins to become mainly inward where it loads salt to cause salt deformation. (**b4**) Magmatic budget (plume intensity) continues to wane to that of normal seafloor spreading (in this model), although at shallower levels than normal (<2.6 km subsea) if the dynamic elevation is not yet fully diminished. Faulting largely ceases at P3 where salt is already thickest, and continued extension is taken up as seafloor spreading at P4–P5. Salt flows under gravity but can also be stretched by late rifting, with 'crept' salt spilling out onto the proximal fringe of the oceanic crust. Shallow water settings may exist out to P3, but basinward halokinesis will increase the average bathymetry of the salt.

**Supplementary Data, Part C. Igneous age compilations, central South Atlantic, providing detail for Figure 6.**

**Supplementary Data, Figs. C1a,b,c**. Same maps as in **Figure 6a,b,c** but showing published or observed (in seismic data) occurrences of igneous activity around the times of each map. Sources of information are tied to the key by symbols, and the references are given below.

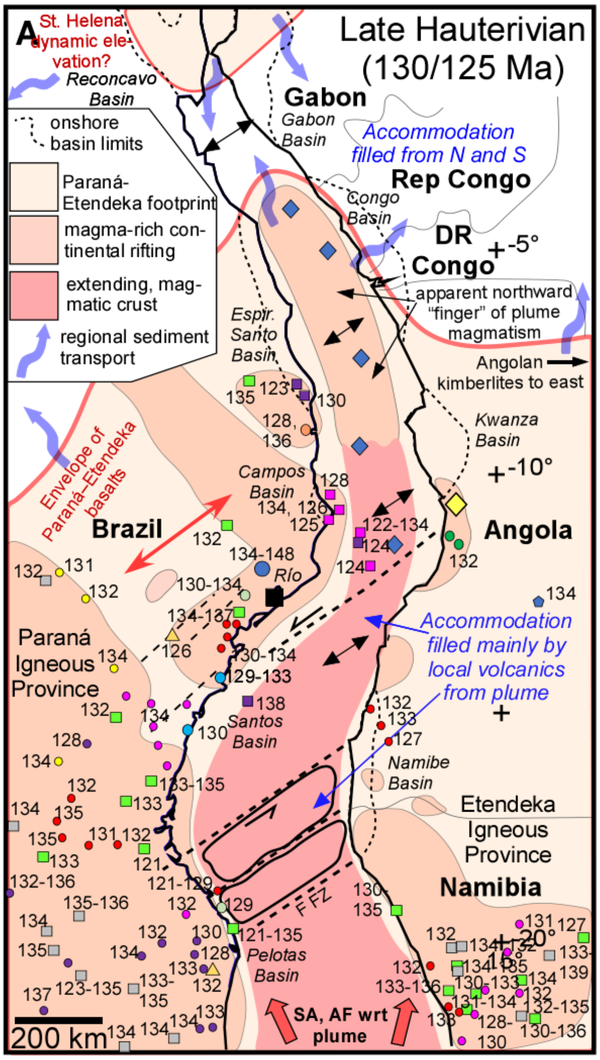


**Map A locales and notes:**

- ■ Fodor *et al.* (1983)
- ■ Mizusaki *et al.* (1992)
- • - Alkaline rocks ($Ar^{40}/Ar^{39}$ ages)
- • -Tholeiitic continental flood basalts, Parana basin;
- • -Tholeiitic dikes structurally below flood basalts;
  All after Gibson (2006)
- • Tholeiitic rocks; de Assis Janasia *et al.* (2011)
- • Tholeiitic rocks ($Ar^{40}/Ar^{39}$ ages); Marzoli *et al.* (1999)
- ◇ 125 Ma dykes; Marzolli *et al.* (1999)
- • Dolerite dike ($Ar^{40}/Ar^{39}$ ages); Turner *et al.* (1995)
- • Tholeiitic dyke swarms; Deckard *et al.* (1998).
- • Novais *et al.* (2004).
- ● Guedes *et al.* (2005)
- △ Lagorio *et al.* (2016)
- ◆ Pre-sag volcanic syn-rift, from seismic interpretation
- ⬟ Castillo-Oliver *et al.* (2016)
- ■ 1 - Low-Ti Gramado and Esmeralda basaltic rocks; 2 - Low-Ti Palmas acidic volcanics; 3 - High-Ti Urubici basalts; 4 - High-Ti Chapeco acidic volcanics; 5 - High-Ti Pitanga basaltic rocks; 6 - High-Ti Paranapanema basaltic rocks. Gomes and Vasconcelos (2021)
- ■ Dykes, sills and subalkaline and alkaline intrusive complexes related to the Parana-Etendeka event in South America. Gomes and Vasconcelos (2021)

**Fig. C1a.**

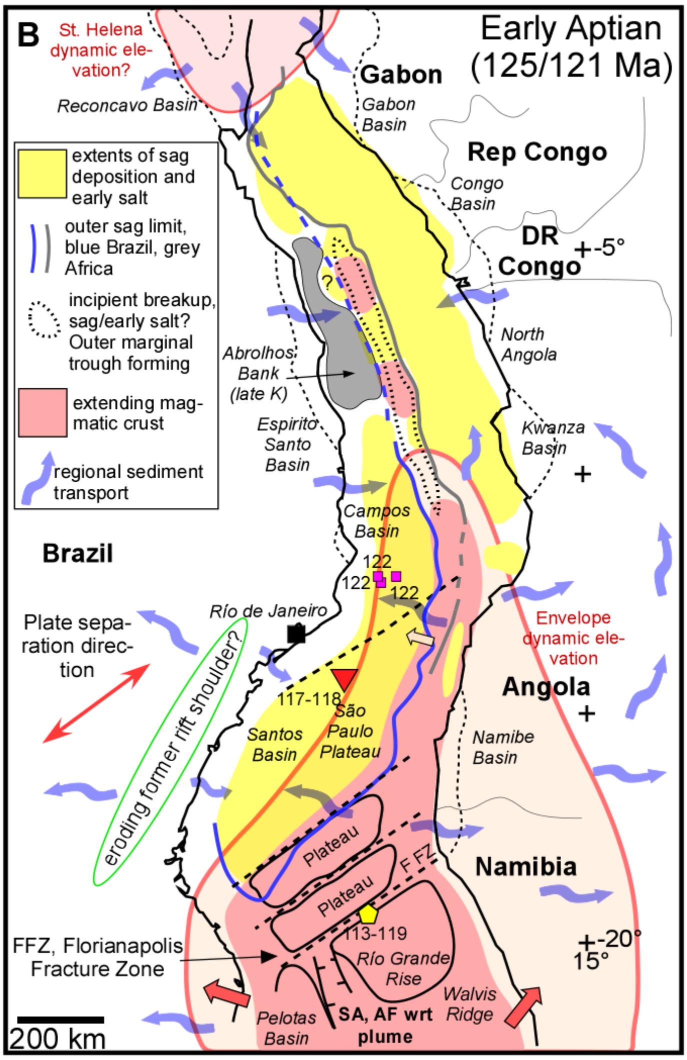


**Map B locales and notes:**

- Basalts constrain age of LES in Santos basin. 117–118 Ma ages (well 1-RJS-625) in the northern Santos Basin at the base of the sag section Moreira *et al.* (2007)
- O'Connor and Duncan (1990)
- Mizusaki *et al.* (1992)

**Figs. C1b.**

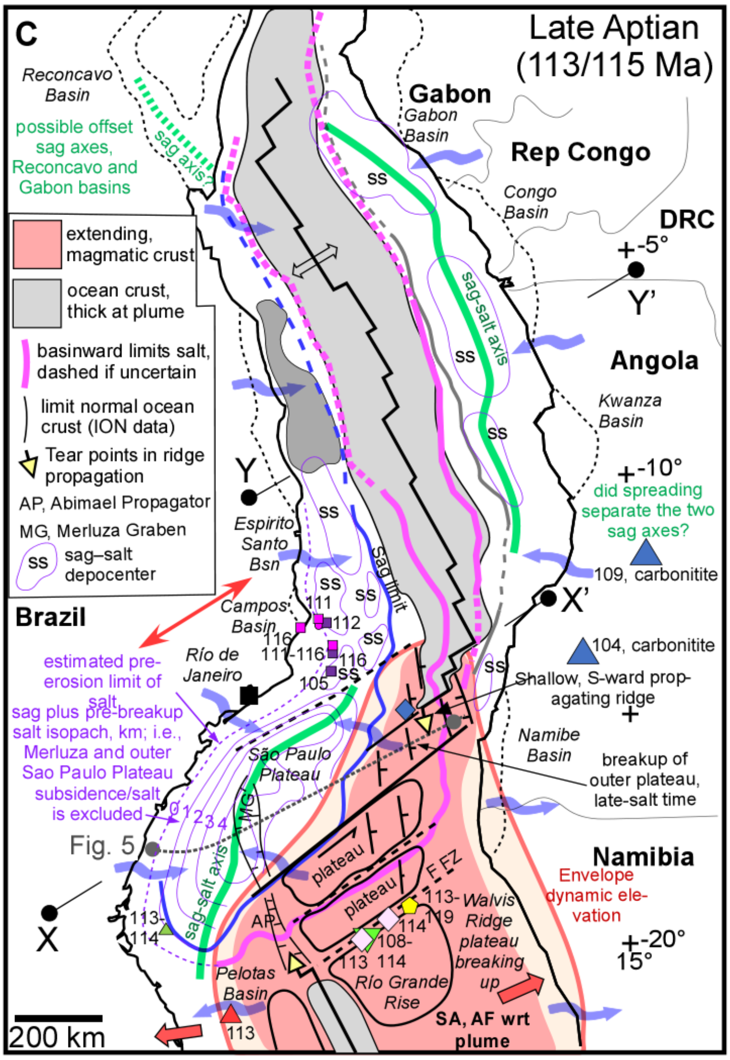


**Map C locales and notes:**

- Fodor *et al.* (1983)
- Mizusaki *et al.* (1992)
- O'Connor and Jokat (2015)
- Tristan / Walvis
  Hoemle *et al.* (2015)
- O'Connor and Duncan (1990)
- Homrighausen *et al.* 2020
- Mizusaki and Saracchine (1990).
- Post-salt volcanic (from seismic observation)
- 113 Ma reported for basalt in well 1-SCS-2 near the top of the LES. The well is located near the west limit of the Florionopolis fracture zone and is overlain by Albian carbonates and anhydrites. It may be a layer near top of salt inside LES. Dias *et al.* (1994)

**Figs. C1c.**

**References cited in Supplementary Data, Part C.**

**References used for the isopach lines of Supplementary Data, Fig. C1c**.

Assine et al. (2008), Contreras et al. (2010), Contreras (2011), de Melo Garcia et al. (2012), Evain et al. (2015), Gomes et al. (2012), Gordon and Mohriak (2015), Jackson et al. (2015), Kumar et al. (2013), Lebit et al. (2019), Pichel et al. (2021), Rodriguez et al. (2018), Zalán and Oliveira (2005), Zalán et al. (2011).

**References used for the igneous ages for Supplementary Data, Part C, including those for the isopach lines in Supplementary Data, Fig. C1c.**


Assine, M.L., Corrêa, F.S. and Chang, H.K. 2008. Migração de depocentros na Bacia de Santos: importância na exploração de hidrocarbonetos. *Revista Brasileira de Geociências*, ***38***(2 suppl), pp.111–127.

Castillo-Oliver, M., Galí, S., Melgarejo, J.C., Griffin, W.L., Belousova, E., Pearson, N.J., Watangua, M. and O'Reilly, S.Y. 2016. Trace-element geochemistry and U–Pb dating of perovskite in kimberlites of the Lunda Norte province (NE Angola): Petrogenetic and tectonic implications. *Chemical geology*, ***426***, pp.118–134. https://doi.org/10.1016/j.chemgeo.2015.12.014

Contreras, J., Zühlke, R., Bowman, S. and Bechstädt, T. 2010. Seismic stratigraphy and subsidence analysis of the southern Brazilian margin (Campos, Santos and Pelotas basins). *Marine and Petroleum Geology*, ***27*****(9),** pp.1952–1980. https://doi.org/10.1016/j.marpetgeo.2010.06.007

Contreras, J., 2011. Seismo-stratigraphy and numerical basin modeling of the southern Brazilian continental margin*. Doctoral dissertation*. *Universität Heidelberg*. 171 p.

de Assis Janasi, V., de Freitas, V.A. and Heaman, L.H. 2011. The onset of flood basalt volcanism, Northern Paraná Basin, Brazil: a precise U–Pb baddeleyite/zircon age for a Chapecó-type dacite. *Earth and Planetary Science Letters*, ***302*****(1–2)**, pp.147–153. https://doi.org/10.1016/j.epsl.2010.12.005

Deckart, K., Féraud, G., Marques, L.S. and Bertrand, H. 1998. New time constraints on dyke swarms related to the Paraná-Etendeka magmatic province, and subsequent South Atlantic opening, southeastern Brazil. *Journal of Volcanology and Geothermal Research*, ***80*****(1–2),** pp.67–83. https://doi.org/10.1016/S0377-0273(97)00038-3

de Melo Garcia, S.F., Letouzey, J., Rudkiewicz, J.L., Danderfer Filho, A. and de Lamotte, D.F. 2012. Structural modeling based on sequential restoration of gravitational salt deformation in the Santos Basin (Brazil). *Marine and Petroleum Geology*, ***35*****(1)**, pp.337–353. https://doi.org/10.1016/j.marpetgeo.2012.02.009

Dias, J.L., Sad, A.R.E., Fontana, R.L., and Feijó, F.J. 1994, Bacia de Pelotas, *Boletim de Geociencias da Petrobras,* **v. 8**, p. 235–245.

Evain, M., Afilhado, A., Rigoti, C., Loureiro, A., Alves, D., Klingelhoefer, F., Schnurle, P., Feld, A., Fuck, R., Soares, J. and De Lima, M.V. 2015. Deep structure of the santos basin-são Paulo plateau system, SE Brazil. *Journal of Geophysical Research: Solid Earth*, ***120*****(8),** pp.5401–5431. https://doi.org/10.1002/2014JB011561

Fodor, R.V., McKee, E.H. and Asmus, H.E. 1983. K-Ar ages and the opening of the South Atlantic Ocean: basaltic rock from the Brazilian margin. *Marine geology*, ***54*****(1–2)**, pp.M1–M8. https://doi.org/10.1016/0025-3227(83)90002-6

Gibson, S.A., Thompson, R.N. and Day, J.A. 2006. Timescales and mechanisms of plume–lithosphere interactions: 40Ar/39Ar geochronology and geochemistry of alkaline igneous rocks from the Paraná–Etendeka large igneous province. *Earth and Planetary Science Letters*, ***251*****(1–2)**, pp.1–17. https://doi.org/10.1016/j.epsl.2006.08.004

Gomes, A.S. and Vasconcelos, P.M. 2021. Geochronology of the Paraná-Etendeka large igneous province. *Earth-Science Reviews*, p.103716. https://doi.org/10.1016/j.earscirev.2021.103716

Gomes, P.O., Kilsdonk, B., Grow, T., Minken, J. and Barragan, R., 2012. Tectonic evolution of the outer high of Santos basin, southern Sao Paulo Plateau, Brazil, and implications for hydrocarbon exploration. *In* D. Gao, ed., *Tectonics and sedimentation: Implications for petroleum systems*: AAPG Memoir **100**, pp.125–142.

Gordon, A.C. and Mohriak, W.U., 2015. Seismic volcano-stratigraphy in the basaltic complexes on the rifted margin of Pelotas Basin, Southeast Brazil. In *34th Annual GCSSEPM Foundation Perkins-Rosen Research Conference, Petroleum Systems in Rift Basins,* Extended Abstracts. pp. 748–786.

Guedes, E., Heilbron, M., Vasconcelos, P.M., de Morisson Valeriano, C., de Almeida, J.C.H., Teixeira, W. and Thomaz Filho, A. 2005. K–Ar and 40Ar/39Ar ages of dikes emplaced in the onshore basement of the Santos Basin, Resende area, SE Brazil: implications for the south Atlantic opening and Tertiary reactivation. *Journal of South American Earth Sciences*, ***18*****(3–4)**, pp.371–382. https://doi.org/10.1016/j.jsames.2004.11.008

Hoernle, K., Rohde, J., Hauff, F., Garbe-Schönberg, D., Homrighausen, S., Werner, R. and Morgan, J.P. 2015. How and when plume zonation appeared during the 132 Myr evolution of the Tristan Hotspot. *Nature Communications*, ***6*****(1)**, pp.1–10. https://doi.org/10.1038/ncomms8799

Homrighausen, S., Hoernle, K., Zhou, H., Geldmacher, J., Wartho, J.A., Hauff, F., Werner, R., Jung, S. and Morgan, J.P. 2020. Paired EMI-HIMU hotspots in the South Atlantic—Starting plume heads trigger compositionally distinct secondary plumes?. *Science Advances*, ***6*****(28),** https://doi.org/10.1126/sciadv.aba0282.

Jackson, C.A.L., Jackson, M.P. and Hudec, M.R. 2015. Understanding the kinematics of salt-bearing passive margins: A critical test of competing hypotheses for the origin of the Albian Gap, Santos Basin, offshore Brazil. *Bulletin*, ***127*****(11–12),** pp.1730–1751. https://doi.org/10.1130/B31290.1

Kumar, N., Danforth, A., Nuttall, P., Helwig, J., Bird, D.E. and Venkatraman, S. 2013. From oceanic crust to exhumed mantle: A 40-year (1970–2010) perspective on the nature of crust under the Santos Basin, SE Brazil. *Geological Society, London, Special Publications*, ***369*****(1),** pp.147–165. https://doi.org/10.1144/SP369.16

Lagorio, S.L., Vizán, H. and Geuna, S.E. 2016. Early Cretaceous Volcanism in Central and Eastern Argentina During Gondwana Break-Up. *SpringerBriefs in Earth System Sciences,* Springer, Cham. 141 p. ISBN : 978-3-319-29591-6. https://doi.org/10.1007/978-3-319-29593-0

Lebit, H., Arasanipalai, S., Tilton, J., Ollagnon, P. and Virlouvet, B. 2019. High-resolution Seismic imaging in the Santos Basin, Brazil and its impact on Salt Mechanics. *16th International Congress of the Brazilian Geophysical Society*, Rio de Janeiro, Brazil. 6 p.

Marzoli, A., Melluso, L., Morra, V., Renne, P.R., Sgrosso, I., D'antonio, M., Morais, L.D., Morais, E.A.A. and Ricci, G. 1999. Geochronology and petrology of Cretaceous basaltic magmatism in the Kwanza basin (western Angola), and relationships with the Paraná-Etendeka continental flood basalt province. *Journal of Geodynamics*, ***28*****(4–5)**, pp.341–356. https://doi.org/10.1016/S0264-3707(99)00014-9

Mizusaki, A.M.P. and Saracchini, F.E. 1990. Catálogo geral de dados geocronológicos da Petrobrás. *Petrobrás/Cenpes Divex/Setec, Rio de Janeiro, Relatório Interno*. pp 1–30.

Mizusaki, A.M.P., Petrini, R., Bellieni, P., Comin-Chiaramonti, P., Dias, J., De Min, A. and Piccirillo, E.M. 1992. Basalt magmatism along the passive continental margin of SE Brazil (Campos Basin). *Contributions to Mineralogy and Petrology*, ***111*****(2)**, pp.143–160. https://doi.org/10.1007/BF00348948

Moreira, J.L.P., Madeira, C.V., Gil, J.A. and Machado, M.A.P. 2007. Bacia de Santos. *Boletim de Geociencias da Petrobras*, ***15*****(2)**, pp.531–549.

Novais, L.C.C., Teixeira, L.B., Neves, M.D., Rodarte, J.B.M., Almeida, J.D. and Valeriano, C.D.M. 2004. Novas ocorrências de diques de diabásio na faixa Colatina-ES: estruturas rúpteis associadas e implicações tectônicas para as bacias de Campos e do Espírito Santo. *Boletim de Geociências da Petrobras*, ***12*****(1),** pp.191–194.

O'Connor, J.M. and Duncan, R.A. 1990. Evolution of the Walvis Ridge-Rio Grande Rise hot spot system: Implications for African and South American plate motions over plumes. *Journal of Geophysical Research: Solid Earth*, ***95*****(B11),** pp.17475–17502. https://doi.org/10.1029/JB095iB11p17475

O'Connor, J.M. and Jokat, W. 2015. Age distribution of Ocean Drill sites across the Central Walvis Ridge indicates plate boundary control of plume volcanism in the South Atlantic. *Earth and Planetary Science Letters*, ***424***, pp.179–190. https://doi.org/10.1016/j.epsl.2015.05.021

Pichel, L.M., Jackson, C.A.L., Peel, F. and Ferrer, O. 2021. The Merluza Graben: How a Failed Spreading Center Influenced Margin Structure, and Salt Deposition and Tectonics in the Santos Basin, Brazil. *Tectonics*, **40**, e2020TC006640. https://doi.org/10.1029/2020TC006640

Rodriguez, C.R., Jackson, C.L., Rotevatn, A., Bell, R.E. and Francis, M. 2018. Dual tectonic-climatic controls on salt giant deposition in the Santos Basin, offshore Brazil. *Geosphere*, ***14*****(1),** pp.215–242. https://doi.org/10.1130/GES01434.1

Turner, J.P. 1995. Gravity-driven structures and rift basin evolution: Rio Muni Basin, offshore equatorial West Africa. *AAPG bulletin*, ***79*****(8),** pp.1138–1158. https://doi.org/10.1306/8D2B21FF-171E-11D7-8645000102C1865D

Zalán, P.V. and Oliveira, J.A. 2005. Origem e evolução estrutural do Sistema de Riftes Cenozóicos do Sudeste do Brasil. *Boletim de Geociencias da Petrobras*, ***13*****(2)**, pp.269–300.

Zalán, P.V., Severino, M.D.C.G., Rigoti, C.A., Magnavita, L.P., Oliveira, J.A.B. and Vianna, A.R. 2011. An entirely new 3D-view of the crustal and mantle structure of a South Atlantic passive margin–Santos, Campos and Espírito Santo basins, Brazil. In *AAPG Annual Conference and Exhibition*, Houston, Texas, Vol. **10**, p. 13.

**Supplementary Data, Part D. Additional seismic reflection data, Gulf of Mexico.**

**Figure Supp Data D1.** 3D line off western Campeche (SD3, see **Figure 8c** of the main paper for location, courtesy of ION). Continental crust is not visible. “Basement” comprises faulted layered igneous flows or SDRs, probably inner SDRs comprising interbedded lava flows and sediments above deeper continental half grabens (true basement). The top of the SDRs defines a top R1 rift unconformity (TRU1). A sag section with little or no magmatism or faulting overlies the TRU1 and approaches 3 km thickness. Basinward this sag section expands and is probably lightly faulted (R2 faults) and intruded by igneous material, and may be fault controlled from off the section, as well. The sag is overlain with no apparent erosion by a base-salt unconformity and an average of 2 km of salt. We consider this margin had a magma-rich syn-rift history, but not enough of the zone of breakup can be seen to comment on the magmatism during breakup.

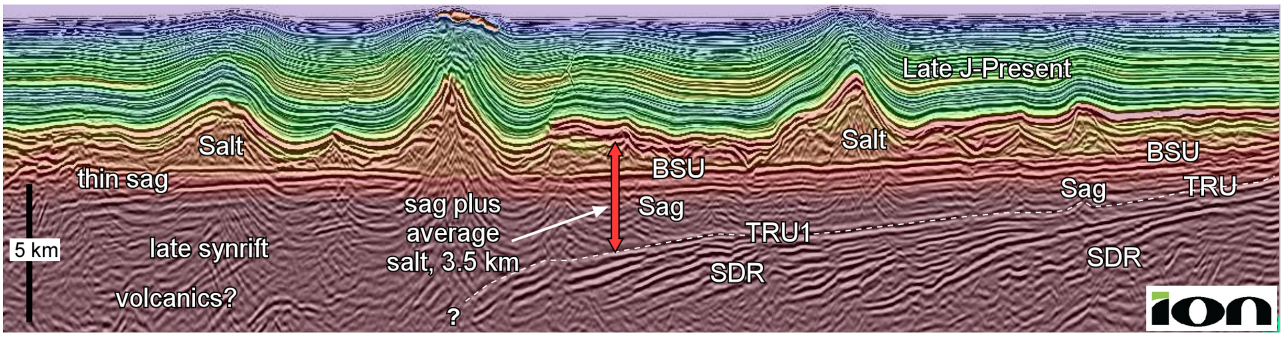

**Supplementary Data, Fig. D2.** MX-080 off NW Yucatán (SD4, see **Figure 8c** of the main paper for location). Thinned continental crust lies at depth and reaches the yellow circle, underlying a thick section of volcano-sedimentary strata with seaward dipping reflector character, probably comprising interbedded lava flows and sediments. In the outer portion of the margin, these strata may reach Moho. This volcano-sedimentary section represents material fill of the R1 syn-rift phase, but serves as basement in the outer margin, posing a semantic issue. There is a base-sag surface that becomes faulted basinward (dashed). The overlying sag section approaches 3 km thickness and shows no magmatism. Basinward, the sag becomes faulted by R2 syn-rift faults. The sag is overlain with no apparent erosion by a base-salt unconformity and an average of 2 km of salt. The sag and base of salt are cut by the outer R2 faults. There is a well-displayed outer marginal detachment (OMD) which relays tectonic extension above. Accepting the outer volcano-sedimentary fill as basement, then basement steps up by ~1 km to the oceanic crust. However, the base of salt steps down to the oceanic crust because the sag is thick, possibly downdip from an important fluvial source. We consider this margin had a magma-rich syn-rift history, but breakup was magma-poor or magma-moderate.

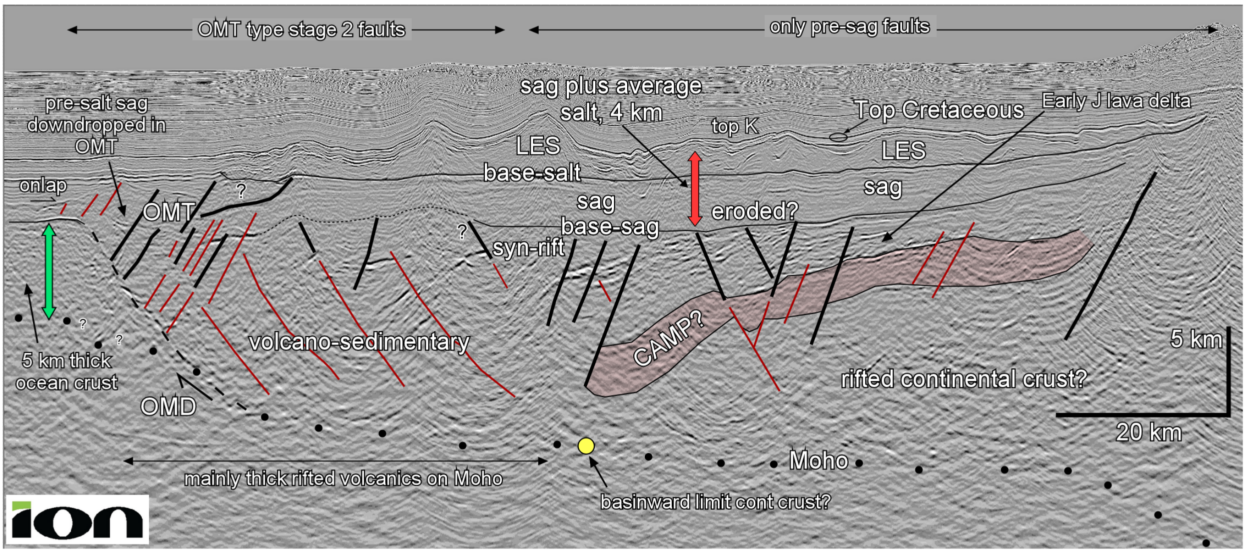

**Supplementary Data, Figs. D3 a–d. (a)** (**c**) ION strike line from the southern North Louisiana Basin showing possible Early Jurassic–Bajocian half graben and sag section above inferred CAMP magmatic level, see **SD 5a** of **Fig. 8c** for location. **(b)** simplified shaded version of **(a). (c,d)** progressive reconstructions of **(b)** to original base level (near sea level) for top and base salt time. The reconstructions were made by slicing the original interpreted line into ~40 vertical strips, and then returning the horizon in question to base level by removing the overburden above the horizon. We estimated the original amount of salt, lost by diapirism and southward draining, by assessing regionals of onlap patterns from numerous surrounding seismic lines (note shown). The analysis shows the perceived R1 rift configuration along the line prior to and after salt deposition. The presence of a thin sag section just beneath the salt is possible, depending on whether the faults drawn were reactivated or are true R1 faults. Our suggestion that the interpreted volcanic section at depth in (**a**) pertains to CAMP magmatism is crucial for the inference that the rifted half graben beneath the salt is Lower Jurassic to Bajocian in age, but this remains unproven. Given the pre-salt geology of the US Gulf margin (e.g. Snedden and Galloway 2019; Frederick et al. 2020 and references in both) an alternative interpretation could be that the rifted half graben structure is middle Triassic in age (related to deposition of the Eagle Mills Formation). However, such an age would not explain the large subsidence observed in the North Louisiana Salt Basin (and other Interior basins) and the US coastal plain. If the faulting were Triassic, the development of Middle Jurassic subsidence would have effectively no faulting or lithospheric attenuation to drive it. Thus, we are confident that the section shows Lower Jurassic–Bajocian rifting.

**References cited in Supplementary Data, Figs. D3a–d**

Frederick, B.C., Blum, M.D., Snedden, J.W. and Fillon, R.H. 2020. Early Mesozoic synrift Eagle Mills Formation and coeval siliciclastic sources, sinks, and sediment routing, northern Gulf of Mexico basin. *GSA Bulletin*, ***132*(11–12),** pp.2631–2650. https://doi.org/10.1130/B35493.1

Snedden, J.W. and Galloway, W.E. 2019. *The Gulf of Mexico Sedimentary Basin Depositional Evolution and Petroleum Applications*. Cambridge University Press, Cambridge, UK. https://doi.org/10.1017/9781108292795

**(a)**

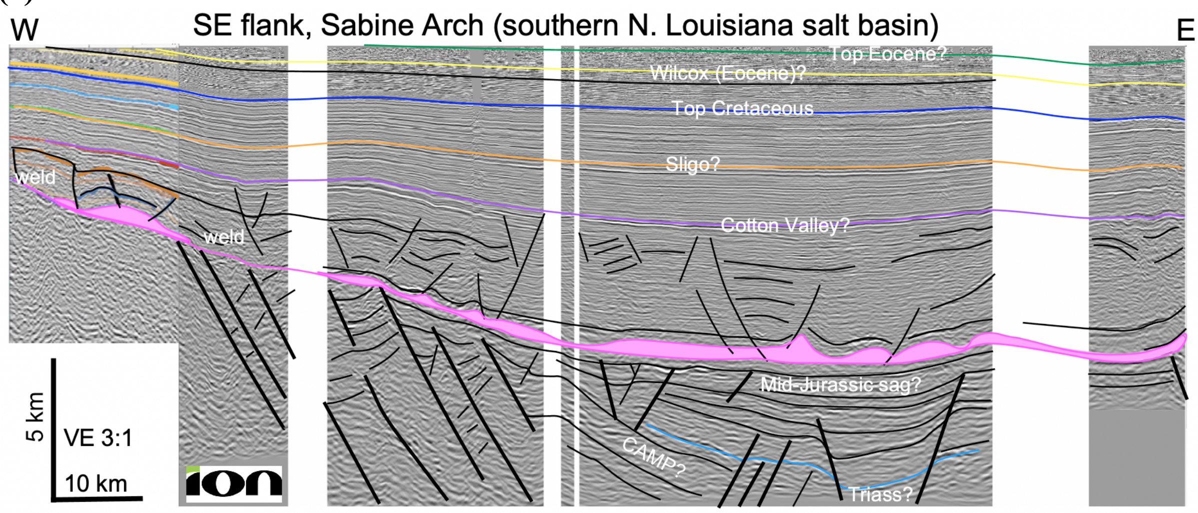

(Figs. D3 b,c,d)

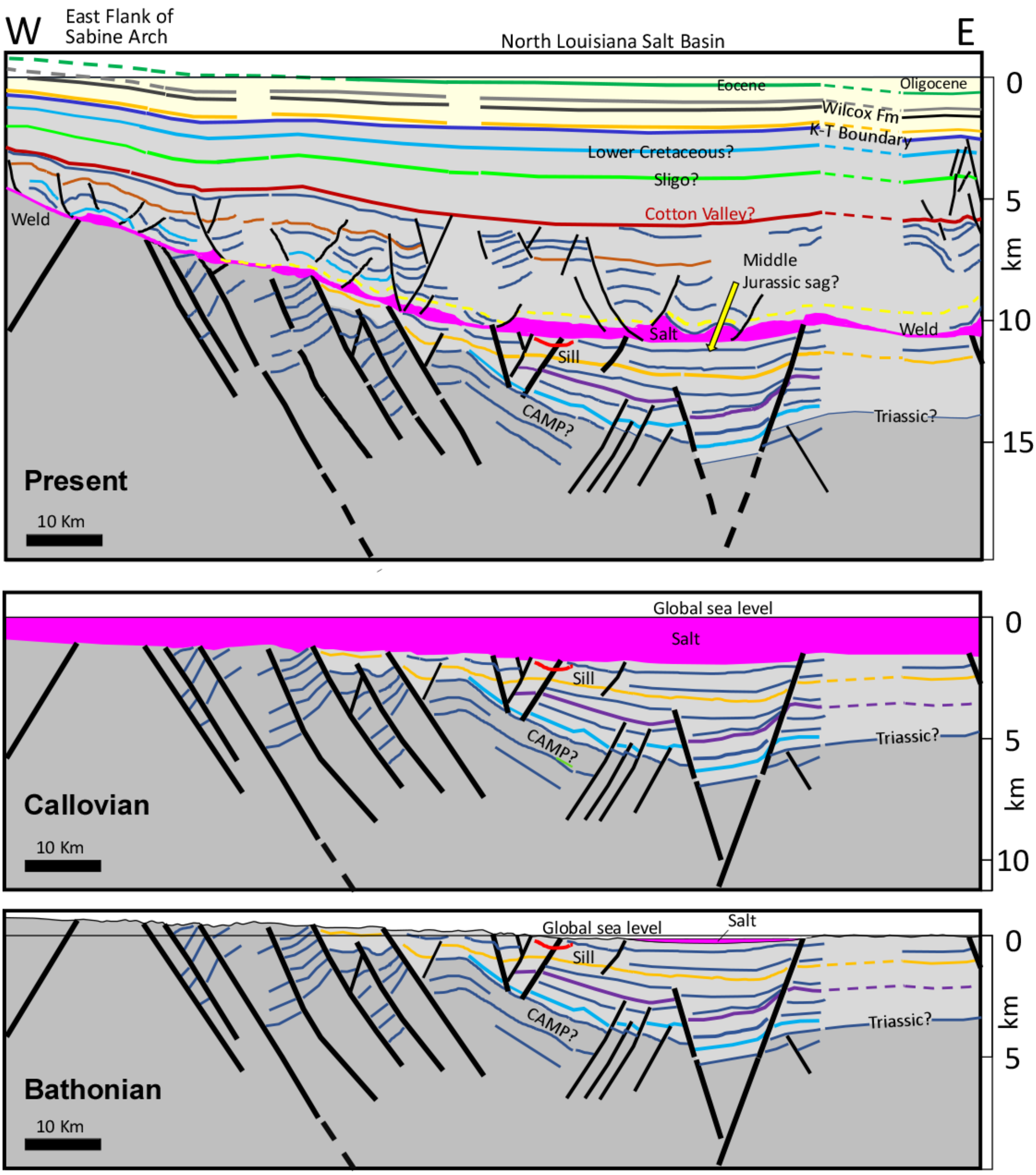
W
East Flank of Sabine Arch
North Louisiana Salt Basin
E
Eocene
Oligocene
Wilcox Fm
K-T Boundary
Lower Cretaceous?
Sligo?
Cotton Valley?
Weld
Middle Jurassic sag?
Salt
Weld
Sill
CAMP?
Triassic?
Present
10 Km
0
5
10
15
km
Global sea level
Salt
Sill
CAMP?
Triassic?
Callovian
10 Km
0
5
10
km
Global sea level
Salt
Sill
CAMP?
Triassic?
Bathonian
10 Km
0
5
km

**Supplementary Data, Part E. Igneous age compilations, Gulf of Mexico, providing detail for Figure 8.**

**Supplementary Data, Figs. E1a–c.** Same maps as in **Figure 8** but showing published or observed (in seismic data) occurrences of igneous activity around the times of each map. Sources of information are tied to the key by symbols. References are given below.

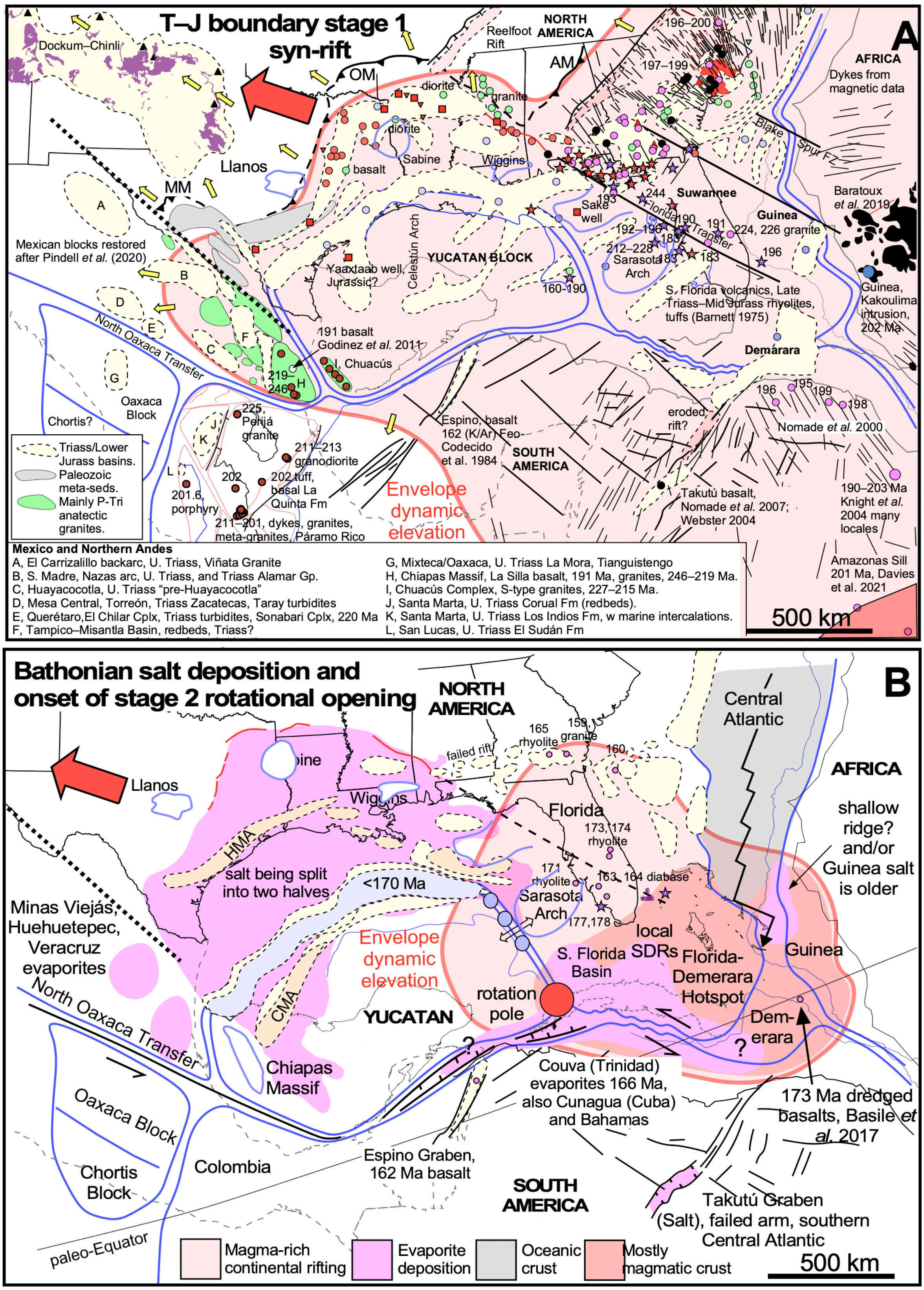

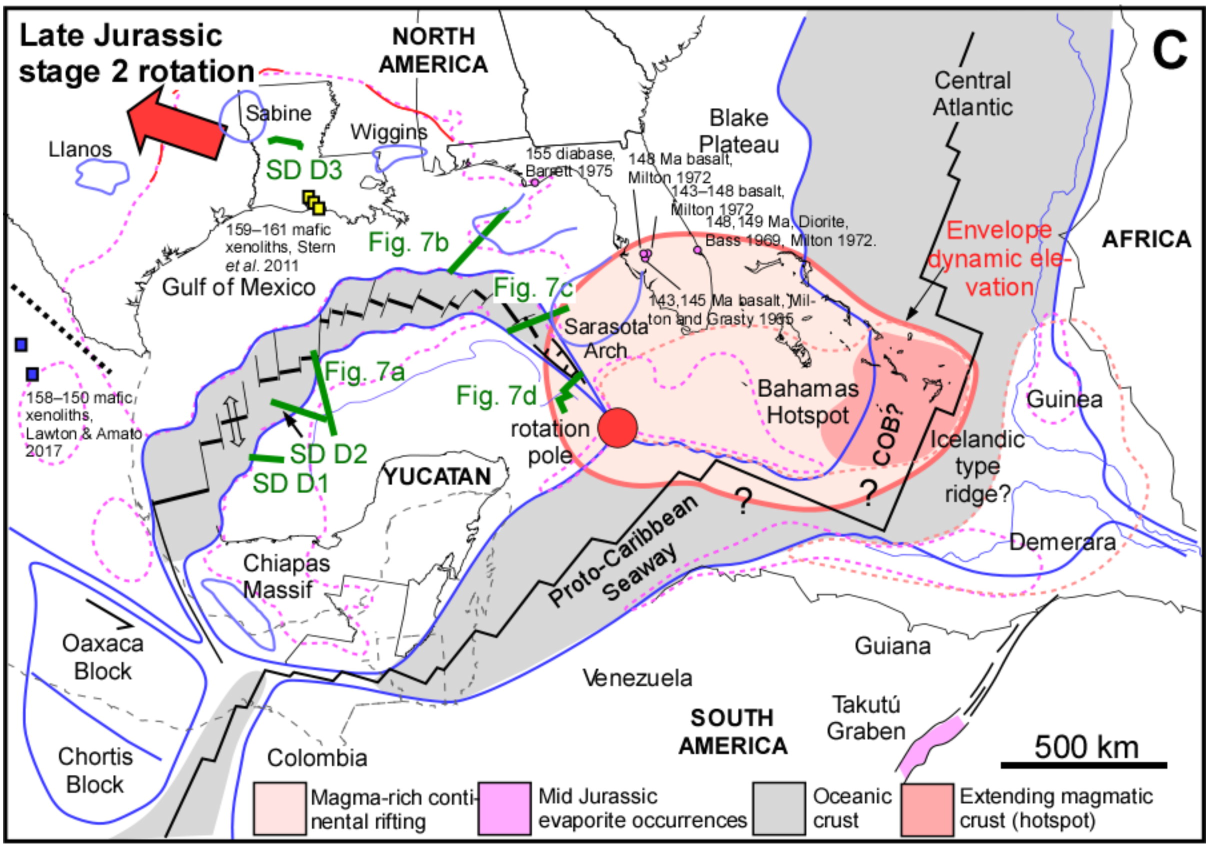


**Ages and distribution of Triassic-Middle Jurassic igneous activity, or strata indicating igneous activity from seismic interpretation, magnetic data, and the literature**

- Ages of igneous rocks (basalts, diabase and felsic volcanics; as reported in Erlich and Pindell (2020).
- Eagle Mills penetrations as reported by Erlich and Pindell (2020).
- Newark Formation penetration from Frederick *et al.* (2020).
- Eagle Mills penetration from Salvador (1991), van Milliken (1988), Frederick *et al.* 2020, respectively.
- Unmetamorphosed, presumed lower Mesozoic (Upper Triassic–Lower Jurassic) syn-rift sedimentary rocks and/or diabase from Benson (1992).
- Early Mesozoic igneous rocks (Byerly 1991).
- CAMP or Triassic rift interpreted on seismic data.
- Basalt penetration (McBride *et al.* 1989; Chowns and Williams 1983).
- Diabase penetration (McBride *et al.* 1989; Chowns and Williams 1983, Nomade *et al.* 2000, 2007).
- Chinli–Dockum zircons from uplifted GoM area (Dickinson *et al.* 2010).
- Dikes from interpretation of magnetic data and from Ragland *et al.* (1983).
- Clubhouse Crossroads Laccolith (Abayrak 2019), “J” reflector is younger, 184 Ma (Lanphere 1983).
- U-Pb ages from CAMP mafic intrusive units (Davies *et al.* 2017) .
- CAMP mafic lava flows (Deckart *et al.* 2005; Davies *et al.* 2017).
- Diabase K–Ar pyroxene age (Barnett 1975; Milton and Grasty 1969).
- From seismic interpretation, intrusions co-eval/younger than salt.
- Salt dome mafic xenoliths, Southern Louisiana (Stern *et al.* 2011)
- Salt dome mafic xenoliths, La Popa Basin (Lawton and Amato 2017)

**References cited in Supplementary Data, Part E.**

**References used for Mexico and the Northern Andes:**

A: Torres et al. (1999), Villarreal-Fuentes et al. (2014) ; B : Barboza-Gudiño et al. (2010), Bartolini (1998), Lawton et al. (2020) ; C : Lawton et al. (2020) ; D : Barboza-Gudiño et al. (2010), Lawton et al. (2020) ; E : Anderson and Schmidt (1983), Ortega-Flores et al. (2014) ; F : Alzaga-Ruiz et al. (2009) ; Cantú-Chapa (1992) ; G : Lawton et al. (2020), Ortega-Flores et al. (2021), Silva-Romo et al. (2015) ; H: Damon et al. (1981), Godínez-Urban et al. (2011), Weber et al. (2005) ; I : Maldonado et al. (2018), Martens et al. (2012), Ratschbacher et al. (2009) ; J, K, L: Bayona et al. (2019), Gómez et al. (2020).

**References used for the igneous ages for Part E.**

Albayrak, K.S. 2019. *3-D* Potential Field Inversion Camp Clubhouse Crossroads Mafic Intrusive Pluton, Coastal Plain, South Carolina. *MSc thesis*, *University of South Carolina*. 67 pp.

Alzaga-Ruiz, H., Lopez, M., Roure, F. and Séranne, M. 2009. Interactions between the Laramide Foreland and the passive margin of the Gulf of Mexico: Tectonics and sedimentation in the Golden Lane area, Veracruz State, Mexico. *Marine and Petroleum Geology*, ***26*****(6)**, pp.951–973. https://doi.org/10.1016/j.marpetgeo.2008.03.009

Anderson, T.H. and Schmidt, V.A. 1983. The evolution of Middle America and the Gulf of Mexico–Caribbean Sea region during Mesozoic time. *Geological Society of America Bulletin*, ***94*****(8),** pp.941–966. https://doi.org/10.1130/0016-7606(1983)94%3C941:TEOMAA%3E2.0.CO;2

Baratoux, L., Söderlund, U., Ernst, R.E., De Roever, E., Jessell, M.W., Kamo, S., Naba, S., Perrouty, S., Metelka, V., Yatte, D. and Grenholm, M. 2019. New U–Pb Baddeleyite Ages of Mafic Dyke Swarms of the West African and Amazonian Cratons: implication for their configuration in supercontinents through time. In *Srivastava R., Ernst R., Peng P. (eds) Dyke Swarms of the World: A Modern Perspective*. Springer Geology. Springer, Singapore. pp. 263–314. https://doi.org/10.1007/978-981-13-1666-1_7

Barnett, R.S. 1975. Basement structure of Florida and its tectonic implications. *Transactions of the Gulf Coast Association of Geological Societies*, 25, pp. 122–142.

Barboza-Gudiño, J.R., Zavala-Monsiváis, A., Venegas-Rodríguez, G. and Barajas-Nigoche, L.D., 2010. Late Triassic stratigraphy and facies from northeastern Mexico: Tectonic setting and provenance. *Geosphere*, *6*(5), pp.621–640. https://doi.org/10.1130/GES00545.1

Bartolini, C., 1998. Stratigraphy, geochronology, geochemistry and tectonic setting of the Mesozoic Nazas Formation, north-central Mexico. *PhD thesis. The University of Texas at El Paso*.

Basile, C., Girault, I., Paquette, J.L., Agranier, A., Loncke, L., Heuret, A. and Poetisi, E. 2020. The Jurassic magmatism of the Demerara Plateau (offshore French Guiana) as a remnant of the Sierra Leone hotspot during the Atlantic rifting. *Scientific reports*, ***10*****(1),** pp.1–12. https://doi.org/10.1038/s41598-020-64333-5

Bass, M.N. 1969. Petrography and ages of crystalline basement rocks of Florida – some extrapolations. AAPG Memoirs, **11**, 283–310

Bayona, G., Bustamante, C., Nova, G. and Salazar Franco, A.M., 2020. Jurassic evolution of the northwestern corner of Gondwana: Present knowledge and future challenges in studying Colombian Jurassic rocks. *In:* Gómez, J. & Pinilla–Pachon, A.O. (editors), *The Geology of Colombia*, Volume 2 Mesozoic. Servicio Geológico Colombiano, Publicaciones Geológicas Especiales 36, p. 171–207. Bogotá. https://doi.org/10.32685/pub.esp.36.2019.05

Benson, R.N. 1992. Map of exposed and buried early Mesozoic rift basins/synrift rocks of the US middle Atlantic continental margin. *Newark, DE: Delaware Geological Survey, University of Delaware.* http://udspace.udel.edu/handle/19716/4289

Byerly, G.R. 1991. Igneous activity. In Salvador, A. *The Gulf of Mexico Basin*. Geological Society of America, The Geology of North America, J, 91–108, https://doi.org/10.1130/DNAG-GNA-J.91

Cantú-Chapa, A. 1992. The Jurassic Huasteca series in the subsurface of Poza Rica, eastern Mexico. *Journal of Petroleum Geology*, ***15*(2),** pp.259–281. https://doi.org/10.1111/j.1747-5457.1992.tb00872.x

Chowns, T.M., Williams, C.T. and Gohn, G.S. 1983. Pre-Cretaceous rocks beneath the Georgia coastal plain—Regional implications. *US Geol. Surv. Prof. Paper*, ***1313***, pp.1–42.

Damon, P.E., Shafiqullah, M. and Clark, K.F. 1981. Evolución de los arcos magmáticos en México y su relación con la metalogénesis. *Revista Mexicana de Ciencias Geológicas*, ***5*(2),** pp.223–238.

Davies, J.H.F.L., Marzoli, A., Bertrand, H., Youbi, N., Ernesto, M. and Schaltegger, U. 2017. End-Triassic mass extinction started by intrusive CAMP activity. *Nature communications*, ***8*(1),** pp.1–8. https://doi.org/10.1038/ncomms15596

Davies, J.H.F.L., Marzoli, A., Bertrand, H., Youbi, N., Ernesto, M., Greber, N.D., Ackerson, M., Simpson, G., Bouvier, A.S., Baumgartner, L. and Pettke, T. 2021. Zircon petrochronology in large igneous provinces reveals upper crustal contamination processes: new U–Pb ages, Hf and O isotopes, and trace elements from the Central Atlantic magmatic province (CAMP). *Contributions to Mineralogy and Petrology*, ***176*(1),** pp.1–24. https://doi.org/10.1007/s00410-020-01765-2

Deckart, K., Bertrand, H. and Liégeois, J.P. 2005. Geochemistry and Sr, Nd, Pb isotopic composition of the central atlantic magmatic province (CAMP) in Guyana and Guinea. *Lithos*, ***82*(3–4),** pp.289–314. https://doi.org/10.1016/j.lithos.2004.09.023

Dickinson, W.R., Gehrels, G.E. and Stern, R.J. 2010. Late Triassic Texas uplift preceding Jurassic opening of the Gulf of Mexico: Evidence from U-Pb ages of detrital zircons. *Geosphere*, ***6*(5)**, pp.641–662. https://doi.org/10.1130/GES00532.1

Erlich, R.N. and Pindell, J. 2021. Crustal origin of the West Florida Terrane, and detrital zircon provenance and development of accommodation during initial rifting of the southeastern Gulf of Mexico and western Bahamas. *Geological Society, London, Special Publications*, ***504*(1)**, pp.77–118. https://doi.org/10.1144/SP504-2020-14

Feo-Codecido, G., Smith, F,D., Aboud, N., de Di Giacomo E. 1984. Basement and Paleozoic rocks of the Venezuelan Llanos basins. In: Bonini, W., Hargraves, R., Shagam, R. *The Caribbean-South American plate boundary and regional tectonics*, **162,** p.175–187. https://doi.org/10.1130/MEM162-p175

Frederick, B.C., Blum, M.D., Snedden, J.W. and Fillon, R.H. 2020. Early Mesozoic synrift Eagle Mills Formation and coeval siliciclastic sources, sinks, and sediment routing, northern Gulf of Mexico basin. *GSA Bulletin*, ***132*(11–12),** pp.2631–2650. https://doi.org/10.1130/B35493.1

Getz, J.E. 2017. The Summerville Formation: Evidence for a sub-horizontal stratigraphic sequence below the post-rift unconformity in the Middleton Place Summerville Seismic Zone. *Doctoral dissertation*, University of South Carolina). 49p.

Godínez-Urban, A., Lawton, T.F., Molina Garza, R.S., Iriondo, A., Weber, B. and López-Martínez, M., 2011. Jurassic volcanic and sedimentary rocks of the La Silla and Todos Santos Formations, Chiapas: Record of Nazas arc magmatism and rift-basin formation prior to opening of the Gulf of Mexico. *Geosphere*, ***7*(1),** pp.121–144. https://doi.org/10.1130/GES00599.1

Gómez, C., Kammer, A., Bernet, M., Piraquive, A. and von Quadt, A. 2021. Late Triassic rift tectonics at the northernmost Andean margin (Sierra Nevada de Santa Marta). *Journal of South American Earth Sciences*, ***105***, p.102953. https://doi.org/10.1016/j.jsames.2020.102953

Knight, K.B., Nomade, S., Renne, P.R., Marzoli, A., Bertrand, H. and Youbi, N. 2004. The Central Atlantic Magmatic Province at the Triassic–Jurassic boundary: paleomagnetic and 40Ar/39Ar evidence from Morocco for brief, episodic volcanism. *Earth and Planetary Science Letters*, ***228*(1–2)**, pp.143–160. https://doi.org/10.1016/j.epsl.2004.09.022

Lanphere, M.A. 1983. 40Ar/39Ar ages of basalt from Clubhouse Crossroads test hole# 2, near Charleston, South Carolina. In Gohn, G.S. (ed). *Studies Related to the Charleston, South Carolina, Earthquake of 1886 – Tectonics and Seismicity*. US Department of the Interior, Geological Survey Professional Paper **1313**, B1–B8.

Lawton, T.F. and Amato, J.M. 2017. U-Pb ages of igneous xenoliths in a salt diapir, La Popa basin: Implications for salt age in onshore Mexico salt basins. *Lithosphere*, **9(5),** pp.745–758. https://doi.org/10.1130/L658.1

Lawton, T.F., Sierra-Rojas, M.I. and Martens, U., 2020. Stratigraphic correlation chart of Carboniferous–Paleogene rocks of Mexico, adjacent southwestern United States, Central America, and Colombia. *In* Martens, U., and Molina Garza, R.S., eds., *Southern and Central Mexico: Basement Framework, Tectonic Evolution, and Provenance of Mesozoic–Cenozoic Basins*, Geological Society of America Special Paper **546**. https://doi.org/10.1130/SPE546

McBride, J.H., Nelson, K.D. and Brown, L.D. 1989. Evidence and implications of an extensive early Mesozoic rift basin and basalt/diabase sequence beneath the southeast Coastal Plain. *Geological Society of America Bulletin*, ***101*****(4)**, pp.512–520. https://doi.org/10.1130/0016-7606(1989)101%3C0512:EAIOAE%3E2.3.CO;2

Maldonado, R., Ortega-Gutiérrez, F. and Ortíz-Joya, G.A. 2018. Subduction of Proterozoic to Late Triassic continental basement in the Guatemala suture zone: A petrological and geochronological study of high-pressure metagranitoids from the Chuacús complex. *Lithos*, ***308*****,** pp.83–103. https://doi.org/10.1016/j.lithos.2018.02.030

Martens, U.C., Brueckner, H.K., Mattinson, C.G., Liou, J.G. and Wooden, J.L. 2012. Timing of eclogite-facies metamorphism of the Chuacús complex, Central Guatemala: record of Late Cretaceous continental subduction of North America's sialic basement. *Lithos*, ***146***, pp.1–10. https://doi.org/10.1016/j.lithos.2012.04.021

Milton, C., 1972. Igneous and metamorphic basement rocks of Florida. Florida Bureau of Geology Bulletin **55**, 125 p.

Milton, C. and Grasty, R. 1969. “Basement” rocks of Florida and Georgia. *AAPG Bulletin*, ***53*****(12),** pp.2483–2493. https://doi.org/10.1306/5D25C96B-16C1-11D7-8645000102C1865D

Nomade, S., Théveniaut, H., Chen, Y., Pouclet, A. and Rigollet, C. 2000. Paleomagnetic study of French Guyana Early Jurassic dolerites: hypothesis of a multistage magmatic event. *Earth and Planetary Science Letters*, ***184*****(1),** pp.155–168. https://doi.org/10.1016/S0012-821X(00)00305-8

Nomade, S., Knight, K.B., Beutel, E., Renne, P.R., Verati, C., Féraud, G., Marzoli, A., Youbi, N. and Bertrand, H. 2007. Chronology of the Central Atlantic Magmatic Province: implications for the Central Atlantic rifting processes and the Triassic–Jurassic biotic crisis. *Palaeogeography, Palaeoclimatology, Palaeoecology*, ***244*****(1–4)**, pp.326–344. https://doi.org/10.1016/j.palaeo.2006.06.034

Ortega-Flores, B., Solari, L., Lawton, T.F. and Ortega-Obregón, C. 2014. Detrital-zircon record of major Middle Triassic–Early Cretaceous provenance shift, central Mexico: Demise of Gondwanan continental fluvial systems and onset of back-arc volcanism and sedimentation. *International Geology Review*, ***56*****(2),** pp.237–261. https://doi.org/10.1080/00206814.2013.844313

Ortega-Flores, B., Solari, L.A. and Martini, M. 2021. Multidimensional Scaling (MDS): A quantitative approximation of zircon ages to sedimentary provenance with some examples from Mexico. *Journal of South American Earth Sciences*, p.103347. https://doi.org/10.1016/j.jsames.2021.103347

Pindell, J., Villagómez, D., Molina-Garza, R., Graham, R., and Weber, B. 2021. A revised synthesis of the rift and drift history of the Gulf of Mexico and surrounding regions in the light of improved age dating of the Middle Jurassic salt, *in* Davison, I., Hull, J., and Pindell, J. (eds.), The Basins, Orogens and Evolution of the Southern Gulf of Mexico and Northern Caribbean, *Geol Soc. London, SP **504***, 29–76, https://doi.org/10.1144/SP504-2020-43

Ratschbacher, L., Franz, L., Min, M., Bachmann, R., Martens, U., Stanek, K., Stübner, K., Nelson, B.K., Herrmann, U., Weber, B. and López-Martínez, M., 2009. The North American-Caribbean plate boundary in Mexico-Guatemala-Honduras. *Geological Society, London, Special Publications*, ***328*****(1),** pp.219–293. https://doi.org/10.1144/SP328.11

Ragland, P.C., Hatcher Jr, R.D. and Whittington, D. 1983. Juxtaposed Mesozoic diabase dike sets from the Carolinas: A preliminary assessment. *Geology*, ***11*****(7)**, pp.394–399. https://doi.org/10.1130/0091-7613(1983)11%3C394:JMDDSF%3E2.0.CO;2

Reid, J.C. and Taylor, K.B. 2015. Mesozoic Rift Basins–Onshore North Carolina and South-Central Virginia, USA: Deep River and Dan River-Danville Total Petroleum Systems (TPS) and Assessment Units (AU) for Continuous Gas Accumulation Atlantic Margins. Extended abstract presented at *CSPG/CSEG/CWLS GeoConvention 2013*, Calgary, Canada. Search and Discovery Article #10712.

Salvador, A. 1991. Triassic–Jurassic. *in* Salvador, A. (ed). *The Gulf of Mexico Basin* Geological Society of America, DNGA Geology of North America, **vol. J**, pp. 131–180. https://doi.org/10.1130/DNAG-GNA-J.131

Silva-Romo, G., Mendoza-Rosales, C.C., Campos-Madrigal, E., Centeno-García, E. and Peralta-Salazar, R. 2015. Early Mesozoic Southern Mexico–Amazonian connection based on U–Pb ages from detrital zircons: The La Mora Paleo-River in the Mixteca Terrane and its paleogeographic and tectonic implications. *Gondwana Research*, ***28*****(2)**, pp.689–701. https://doi.org/10.1016/j.gr.2014.06.005

Stern, R.J., Anthony, E.Y., Ren, M., Lock, B.E., Norton, I., Kimura, J.I., Miyazaki, T., Hanyu, T., Chang, Q. and Hirahara, Y. 2011. Southern Louisiana salt dome xenoliths: First glimpse of Jurassic (ca. 160 Ma) Gulf of Mexico crust. *Geology*, **39(4),** pp.315–318. https://doi.org/10.1130/G31635.1

Torres, R., Ruiz, J., Patchett, P.J., Grajales, J.M., Bartolini, C., Wilson, J.L. and Lawton, T.F. 1999. A Permo-Triassic continental arc in eastern Mexico: Tectonic implications for reconstructions of southern North America. *Special Papers-Geological Society of America*, **340,** pp.191–196. https://doi.org/10.1130/0-8137-2340-X.191

Van Milliken, J. 1988. Late Paleozoic and early Mesozoic geologic evolution of the Arklatex area. *Doctoral dissertation, Rice University*. 577 p.

Villarreal-Fuentes, J., Levresse, G., Nieto-Samaniego, A.F. and Corona-Esquivel, R. 2014. New geological and geochronological data of the Placer de Guadalupe uplift, Mexico: a new piece of the Late Triassic–Jurassic Nazas Arc?. *International Geology Review*, ***56*****(16),** pp.2000–2014. https://doi.org/10.1080/00206814.2014.984353

Weber, B., Cameron, K.L., Osorio, M. and Schaaf, P. 2005. A Late Permian tectonothermal event in Grenville crust of the southern Maya terrane: U-Pb zircon ages from the Chiapas Massif, southeastern Mexico. *International Geology Review*, ***47*****(5),** pp.509–529. https://doi.org/10.2747/0020-6814.47.5.509

Webster, R.E. 2004. Tropical versus Temperate Zone Lacustrine Source Rocks: Examples from Takutu Basin, Guyana, and General Levalle Basin, Argentina. Abstract and posters (4) presented at *AAPG Annual Convention*, Dallas, Texas. Search and Discovery Article #10070.

**Supplementary Data, Part F. Iceland as a quasi-analogue for the São Paulo Plateau.**

**Supplementary Data, Fig. F1** shows Iceland as a subaerial NE-SW trending portion of the mid-Atlantic Ridge, elevated by above-average magmatism and dynamic uplift, both caused by a deep mantle plume (Schoonman et al. 2017; Barnett-Moore et al. 2017). Iceland has a central axial zone of extensional faulting and magmatism (Árnason 2020) between relatively dormant onshore zones where erosion and deposition control relief at least as much as active rifting. These onshore zones transition offshore where subsidence outpaces magmatic growth or dynamic uplift. Given this tectonic setting where plume magmatism, dynamic uplift and rifting of thick magmatic crust co-exist, both thermal and dynamic subsidence should be operating at the flanks of Iceland, whereas the onshore rift axis should be heavily influenced by tectonic subsidence, while being held high by dynamic uplift.

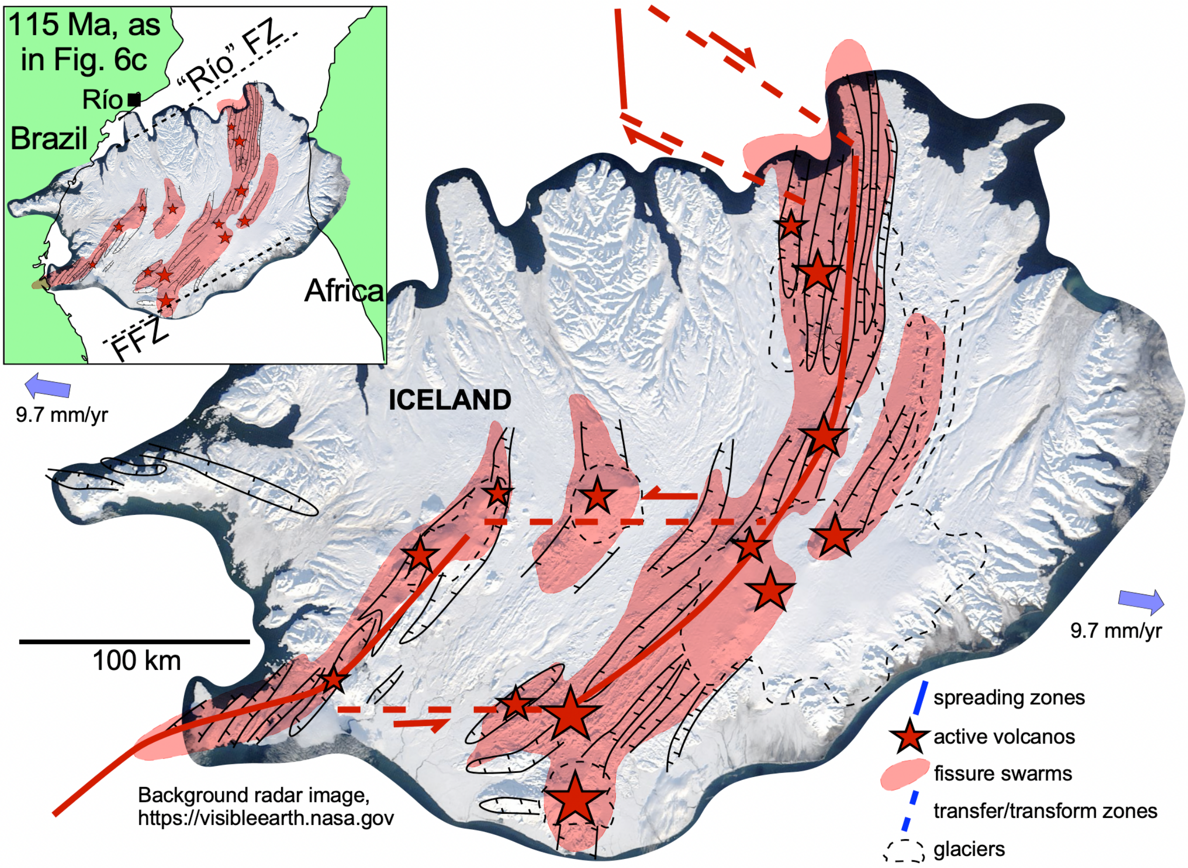


How would Iceland evolve if the plume-driven excess magmatic supply and dynamic uplift drastically waned while tectonic extension continued? We suggest the regional Iceland high would subside by a combination of dynamic (dissipation of the dynamic uplift) and thermal subsidences, i.e. the dynamo-thermal curve in **Fig. 4**, and that the central rift axis would subside even faster due to ongoing tectonic subsidence. Fault motions responsible for that extension and subsidence would post-date most magmatism. If we considered such a setting within a restricted evaporite basin such as the central South Atlantic, salt precipitation would begin while the magmatic crust was still near sea level. Salt's fast potential rate of precipitation could allow deposition to keep pace with the three combined subsidences in the rift axis. The result would be rapid (faster than allowed by thermal subsidence alone) accumulation of shallow water salt on the little-faulted flanks of the central rift axis, and *extremely* rapid accumulation of salt within the central rift axis. With a lack of magmatism, the central rift axis could extend during continued salt deposition to a condition of very thin crust, and subside to an isostatic level approaching that of mantle covered to global sea level by salt, which would be on the order of 8 km.

We contend that this scenario is effectively that which we have interpreted for the early São Paulo Plateau (zones 3 and 4 of **Fig. 5**), following continental breakup when the magmatic plateau filled the void between the continental limits of Brazil and Africa (**Fig. 6c,d**). **Figures 6e,f** complete the breakup picture further, integrating the African margin using ION CongoSPAN data.

**References cited in Supp. Data Part F:**


Árnason, K. 2020. New conceptual model for the magma–hydrothermal–tectonic system of Krafla, NE Iceland. Geosciences, 10, 34, https://doi.org/10.3390/geosciences10010034

Barnett-Moore, N., Hassan, R., Flament, N. and Müller, D. 2017. The deep Earth origin of the Iceland plume and its effects on regional surface uplift and subsidence. Solid Earth, 8, 235–254, https://doi.org/10.5194/se-8-235-2017

Schoonman, C.M., White, N.J. and Pritchard, D. 2017. Radial viscous fingering of hot asthenosphere within the Icelandic plume beneath the North Atlantic Ocean. Earth and Planetary Science Letters, 468, 51–61, https://doi.org/10.1016/j.epsl.2017.03.036